DALTON
FULL PAPER

Magnetostructural characterisation of two M–NCO–bpa polymers (M = Co, Mn and bpa = 1,2-bis(4-pyridyl)ethane)†

Margarita L. Hernández,[a] M. Karmele Urtiaga,[b] M. Gotzone Barandika,[c] Roberto Cortés,*[c] Luis Lezama,[a] Noelia de la Pinta,[c] M. Isabel Arriortua[b] and Teófilo Rojo*[a]

[a] *Departamento de Química Inorgánica, Facultad de Ciencias, Universidad del País Vasco, Apdo. 644, Bilbao 48080, Spain. E-mail: qiproapt@lg.ehu.es*
[b] *Departamento de Mineralogía-Petrología, Facultad de Ciencias, Universidad del País Vasco, Apdo. 644, Bilbao 48080, Spain*
[c] *Departamento de Química Inorgánica, Facultad de Farmacia, Universidad del País Vasco, Apdo. 450, Vitoria 01080, Spain*

Received 6th February 2001, Accepted 1st August 2001
First published as an Advance Article on the web 24th September 2001

The combination of bpa with the pseudohalide cyanate (NCO^-) leads to the preparation of two new isomorphous compounds exhibiting the formula $[M(NCO)_2(bpa)_2]_n \cdot bpa$ where M = Co (**1**), Mn (**2**). Both of them have been magnetostructurally characterised by means of X-ray diffraction analysis, TG measurements, IR and ESR spectroscopies and measurements of the magnetic susceptibility. Both compounds consist of M–(*gauche*-bpa)$_2$–M chains connected through H-bonds. The resulting network shows pseudo-channels (8.5 Å × 9.3 Å). The structure also exhibits *anti*-bpa groups performing as crystallisation molecules that are perpendicularly disposed to the pseudo-channels. Both compounds exhibit antiferromagnetic interactions through metallic centres.

Introduction

The dipyridyl organic ligands are well-known to be excellent spacers for the preparation of coordination polymers. In this context, 4,4′-bipyridine has been extensively used giving rise to a large number of high-dimensional frameworks.[1] The efficiency of this ligand as a mediator between the metallic ions lies in the 4,4′-relative position of the N donor atoms that provide the extension of the polymers.

Further research in this area has been devoted to other dipyridyl ligands[2] that exhibit the 4,4′-relative position of the N atoms but possess several R groups linking both pyridyl rings (Scheme 1(a)). Obviously, each py–R–py ligand exhibits not

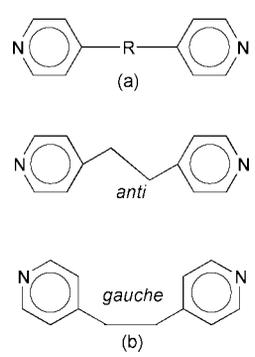

Scheme 1

only a distinct N–N′ distance but also other distinguishing characteristics. Among them, the rigidity of some of these ligands is a clear limiting factor for a self-assembly strategy for the synthesis of polymeric compounds. Therefore, the use of flexible linkers like 1,2-bis(4-pyridyl)ethane (bpa) seems to be specially convenient.

† Electronic supplementary information (ESI) available: powder XRD data for compound **2**. See http://www.rsc.org/suppdata/dt/b1/b101192h/

As a consequence of the freedom of rotation exhibited by the ethyl group, bpa can adopt two different conformations, *anti* and *gauche* (Scheme 1(b)), both conformers being able to perform as co-ordinating ligands (either bridging or terminal) and/or as crystallisation molecules. As a result, bpa is characterised by a remarkably high capability to become accommodated in the structural framework, making it an excellent candidate for the preparation of co-ordination polymers. Several bpa-polymers have been reported over the last few years, illustrating the potential of this ligand in this context.[3]

Our previous work with bpa concerned two families of 1D and 2D compounds[4] where this ligand is combined with ambidentate pseudohalides (L = N_3, NCS). Both sets of compounds ($[ML_2(bpa)_n]_n$, where M is a divalent cation and n = 1,2) exhibit bpa just as a bridging ligand. In this paper, we report on two new isomorphous compounds where bpa groups not only perform as co-ordinating ligands but also as crystallisation molecules. Both compounds exhibit the formula $[ML_2(bpa)_2]_n \cdot$ bpa where M = Co (**1**), Mn (**2**) and L = NCO. The complex part of these compounds exhibit pseudo-channels formed by the packing of M–(bpa)$_2$–M linear chains. The crystallisation molecules of bpa are perpendicularly disposed to these pseudo-channels.

Experimental

Syntheses

Synthesis of compound **1** was carried out by adding an aqueous solution of KNCO (2.5 mmol) to an aqueous solution of $Co(SO_4)_2 \cdot 7H_2O$ (0.5 mmol). After one hour stirring a warm ethanolic solution of bpa (1.5 mmol) was added to this mixture. After five hours stirring at 50 °C, the resulting solution was left to stand at room temperature. Several days later, prismatic, pink, X-ray quality single crystals were obtained (35% yield).

Compound **2** was similarly synthesised but using $Mn(SO_4)_2 \cdot H_2O$ (0.5 mmol). In this case, pale yellow crystals were obtained

 DOI: 10.1039/b101192h

after several days (53% yield) but they were not good enough for single crystal X-ray analysis. Unfortunately, further attempts to recrystallise this product did not lead to better crystals.

Elemental analysis and atomic absorption results were in good agreement with the $MC_{38}N_8H_{36}O_2$ (M = Co, Mn) stoichiometry for both compounds. Found (calc.): Co, 8.43 (8.47); N, 16.36 (16.11); C, 65.14 (65.61); H, 4.93 (5.21)% for **1**: Mn, 8.12 (7.94); N, 16.47 (16.20); C, 65.44 (65.99); H, 5.38 (5.2)% for **2**:

TG curves obtained for **1** and **2** (25–500 °C) showed that, as reported for similar compounds,[1a,4a] both of them undergo pyrolysis of the ligands, taking place in two steps. The first step, which corresponds to a weight loss of 52.1 (**1**) and 54.1% (**2**), is centred at 180 (**1**) and 170 °C (**2**) and can be attributed to two molecules of bpa per formula unit. The second step (weight loss of 31.8 (**1**) and 34.1% (**2**)) takes place at around 350 (**1**) and 320 °C (**2**). The identification of the final residues was not possible due to the low crystallinity of the samples.

Physical measurements

Microanalyses were performed with a Perkin-Elmer 2400 analyser. Analytical measurements were carried out in an ARL 3410 + ICP with Minitorch equipment. TG curves were obtained using a TA-Instruments SDT-2960 DSC-TGA unit at a heating rate of 5 °C min^{-1} in argon. IR spectroscopy was performed on a Nicolet 520 FTIR spectrophotometer in the 400–4000 cm^{-1} region. Diffuse reflectance spectra were registered at room temperature on a CARY 2415 spectrometer in the range 5000–45000 cm^{-1}. Magnetic susceptibilities of powdered samples were carried out in the temperature range 1.8–300 K (at a value of 1000 Gauss) using a Quantum Design Squid MPM5-7 magnetometer, equipped with a helium continuous-flow cryostat. The experimental susceptibilities were corrected for the diamagnetism of the constituent atoms (Pascal tables).

Crystal structure determination

Single crystal X-ray measurements for compound **1** were taken at room temperature on an Enraf-Nonius CAD-4 diffractometer with graphite-monochromated Mo-K_α radiation (λ = 0.71070 Å), operating in $\omega/2\theta$ scanning mode using suitable crystals for data collection. Accurate lattice parameters were determined from least-squares refinement of 25 well-centred reflections. Intensity data were collected in the θ range 1–30°. During data collection, two standard reflections periodically observed showed no significant variation. Corrections for Lorentz and polarisation factors were applied to the intensity values.

The structure was solved by heavy-atom Patterson methods using the program SHELXS97[5] and refined by a full-matrix least-squares procedure on F^2 using SHELXL97.[6] Non-hydrogen atomic scattering factors were taken from *International Tables of X-Ray Crystallography*.[7] In Table 1, crystallographic data and processing parameters for compound **1** are shown.

CCDC reference number 158590.

See http://www.rsc.org/suppdata/dt/b1/b101192h/ for crystallographic data in CIF or other electronic format.

X-Ray powder diffraction data for compound **2** were collected on a PHILIPS X'PERT powder diffractometer with Cu-K_α radiation in steps of 0.02° over the 5–60° 2θ-angular range and a fixed-time counting of 4 s at 25 °C. The powder diffraction patterns were indexed with the FULLPROF[8] program based on the Rietveld method[9] using the Profile Matching option. Structural data and processing parameters for **2** are given in Table 2.

Table 1 Crystal data and structure refinement for compound **1**

Formula	$CoC_{38}N_8H_{36}O_2$	Z	4
M	695.7	T/°C	20
Crystal system	Monoclinic	λ/Å [a]	0.71070
Space group	C_2/c	ρ_{obs}/g cm^{-3}	1.31(3)
a/Å	19.869(2)	ρ_{cal}/g cm^{-3}	1.288
b/Å	9.639(2)	μ/cm^{-1}	5.23
c/Å	18.821(2)	Unique data	5252
β/°	95.72(2)	Observed data	3227
U/Å^3	3586.6(9)	R (R') [b]	0.0628 (0.1458)

[a] Mo-Kα radiation, graphite monochromator. [b] $R = [\Sigma||F_o| - |F_c||/\Sigma|F_o|]$, $R' = [\Sigma[w(F_o^2 - F_c^2)^2]/\Sigma[w(F_o^2)^2]]^{1/2}$ where $w = 1/\sigma^2(|F_o|)$.

Table 2 Structural data and refinement for compound **2**

Formula	$MnC_{38}N_8H_{36}O_2$	β/°	95.63(9)
M	691.7	U/Å^3	3690.8(3)
Crystal system	Monoclinic	T/°C	25
Space group	C_2/c	λ/Å	1.54056
a/Å	19.967(5)	Rp [a]	8.78
b/Å	9.841(2)	Rwp [b]	12.0
c/Å	18.873(4)	GOF	2.22

[a] $Rp = 100[\Sigma|y_o - y_c|]/\Sigma|y_o|$. [b] $Rwp = [\Sigma[w|y_o - y_c|^2]/\Sigma[w|y_o|^2]]^{1/2}$.

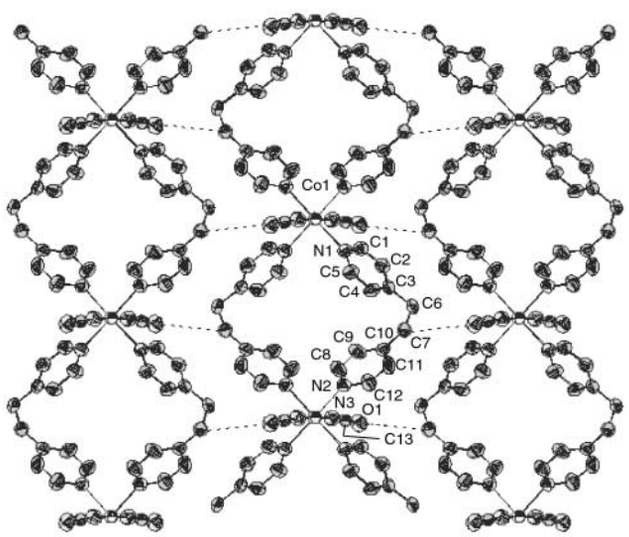

Fig. 1 ORTEP[13] view (50% probability) of the chains of **1** packed on the xy plane. The discontinuous lines represent H-bonds.

Results and discussion

Structural analysis

Compound **1** consists of linear Co–$(bpa)_2$–Co chains extending along the [010] direction that are packed along the xy planes (Fig. 1). The four bpa ligands that are linked to each octahedral Co^{II} adopt the *gauche* conformation providing an intermetallic distance of 9.639 Å. These ligands are located on the equatorial positions of the co-ordination sphere, the axial positions being occupied by terminal N-co-ordinated cyanate groups. While the metallic cations are situated on the same plane, one of the bpa groups and one of the NCO ligands are directed upwards from the plane, the remaining ones being directed downwards. Fig. 1 also shows the H-bonds between the O_{NCO} and the C atoms of the ethane groups of the bpa ligands. The H-bonds, together with some selected parameters for **1**, are displayed in Table 3. As seen, Co–N_{NCO} distances (2.066(3) Å) are slightly shorter than the Co–N_{bpa} distances (2.200(3) Å, on average). On the other hand, the bond angles associated with the co-ordination sphere are very close to the ideal ones. The NCO ligands are nearly linear (N–C–O angle is 178.5(4)°) and the py–C–C–py torsion angle for the co-ordinated bpa groups is 66.3°. Similar

Table 3 Selected bond distances (Å) and angles (°) and most important intermolecular H-bonds (donor · · · acceptor < 3.5 Å) for compound **1**

Co(1)–N(1)	2.196(3)	N(3)–C(13)	1.158(4)		
Co(1)–N(2ii)	2.204(3)	C(13)–O(1)	1.198(4)		
Co(1)–N(3)	2.066(3)				
N(1)–Co(1)–N(1i)	90.8(1)	N(3i)–Co(1)–N(2ii)	89.7(1)		
N(1)–Co(1)–N(2iii)	89.8(1)	N(3)–Co(1)–N(2ii)	91.5(1)		
N(1)–Co(1)–N(2ii)	177.5(1)	N(2ii)–Co(1)–N(2iii)	89.6(2)		
N(3iii)–Co(1)–N(3)	178.3(2)	C(13)–N(3)–Co(1)	167.5(3)		
N(3i)–Co(1)–N(1)	87.8(1)	N(1i)–Co(1)–N(2iii)	177.5(1)		
N(3)–Co(1)–N(1)	91.0(1)	N(3)–C(13)–O(1)	178.5(4)		
Intermolecular H-bonds					
C7–H7A	0.966(9)	C7–O1(iv)	3.456(5)	H7A · · · O1(iv)	2.701(4)
C15–H15	0.90(5)	C15–O1(iii)	3.499(5)	H15 · · · O1(iii)	2.66(5)
C2–H2	0.93(3)	C2–N4(iv)	3.444(5)	H2 · · · N4(iv)	2.76(3)
C7–H7A · · · O1(iv)	135(3)	C15–H15 · · · O1(iii)	155(4)	C2–H2 · · · N4(iv)	131(3)

Symmetry transformations used to generate equivalent atoms: (i) $-x, y, -z + 1/2$; (ii) $-x, y + 1, -z + 1/2$; (iii) $x, y + 1, z$; (iv) $x - 1/2, y - 1/2, z$.

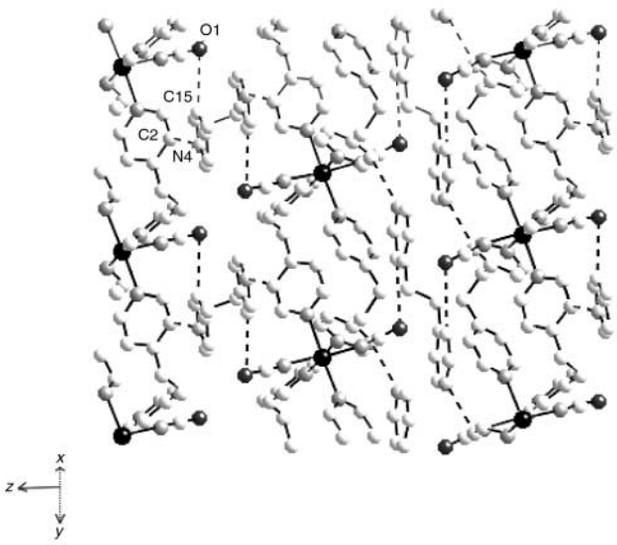

Fig. 2 (110) view of the structure for **1**. The discontinuous lines represent H-bonds.

low values of the torsion angles have been found for other M–(*gauche*-bpa)$_2$–M chains.[3k,4a]

The Co–(bpa)$_2$–Co chains are disposed along *xy* planes that are packed along *z* as shown in Fig. 2. Thus, there are *xy* planes of crystallisation with bpa molecules located between the planes of Co–(bpa)$_2$–Co chains. These bpa groups, adopting the *anti* conformation with a torsion angle of 179.9°, are disposed along the [110] and [1−10] directions in alternate planes. The resulting arrangement provides a highly efficient filling of the space that is based on a great number of H-bonds (Table 3).

The relative shift of the chains along both *x* and *z* directions produces pseudo-channels (8.5 Å × 9.3 Å) along the [10−1] direction. The bpa planes intersect these pseudo-channels as shown in Fig. 3, giving rise to cavities. However, this compound is not sufficiently robust to be considered a proper microporous compound since, as mentioned before, decomposition starts at low temperature as a consequence of the fact that the 3D framework is based on H-bonds.

The powder X-ray diffraction pattern for compound **2** is very similar to the theoretical pattern generated for compound **1**. Therefore, the values corresponding to the cell parameters and space group of compound **1** were used as initial data for the refinement of the experimental patterns for compound **2**. The experimental, calculated (according to the best fit parameters shown in Table 2) and difference patterns are shown in Fig. 4 for compound **2**. These results clearly indicate that compounds

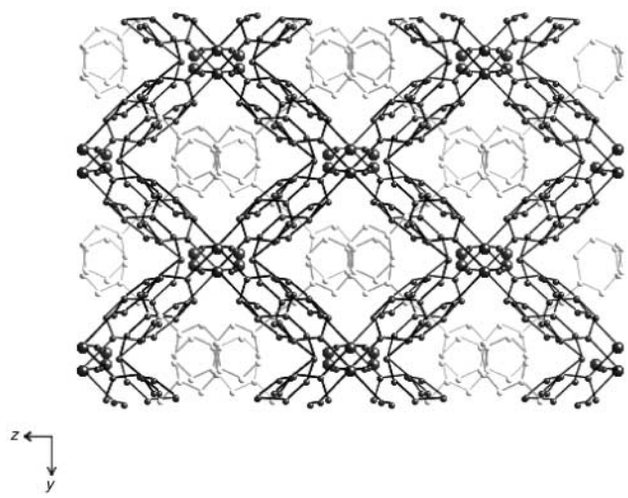

Fig. 3 (10−1) view of the structure for **1** showing the existence of pseudo-channels formed by the complex part of the compound (dark) and the intersecting planes of bpa crystallisation molecules (light).

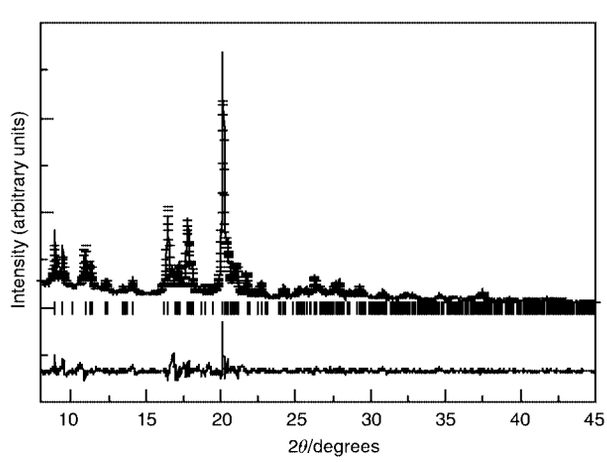

Fig. 4 Experimental, calculated and difference powder X-ray diffraction patterns for **2**.

1 and **2** are isomorphous. The isomorphism of **1** and **2** is also confirmed by the rest of the techniques used in this work.

IR and UV-VIS spectroscopies

A summary of the most important IR bands corresponding to compounds **1** and **2** together with their tentative assignments[10] is given in Table 4. As can be seen, both spectra exhibit an intense absorption at about 2200 cm^{-1} which is associated with the asymmetric stretching mode of the cyanate ligand.

Table 4 Selected IR bands for bpa and $[Co(NCO)_2bpa_2]\cdot bpa$ (**1**) and $[Mn(NCO)_2bpa_2]\cdot bpa$ (**2**), together with their assignments

	bpa	$[Co(NCO)_2bpa_2]\cdot bpa$	$[Mn(NCO)_2bpa_2]\cdot bpa$
Cyanate, ν_{as}(CN)	—	2206s	2199s
Cyanate, ν_s(CN)	—	1300	1301
Cyanate, δ	—	617	618
Pyridyl ring stretching, ν(C=C)	1594	1612	1612
ν(ArC–C, C=N)	1413	1419	1419
Pyridyl ring breathing, δ(ArC–H)	982	1016	1016
Pyridyl out of plane bending, ν(ArC–H)	817	828	828
Pyridyl ring in plane vibration	539	550	548

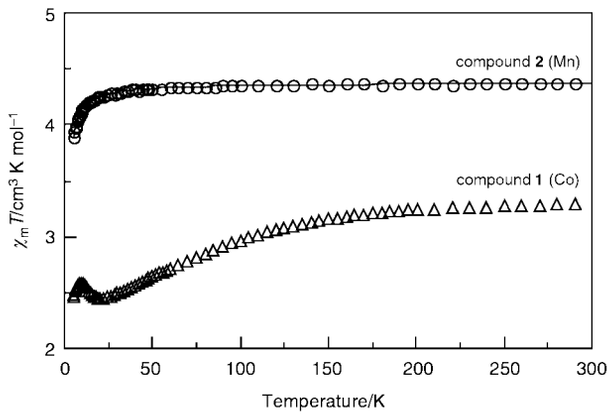

Fig. 5 Thermal evolution of $\chi_m T$ for compounds **1** and **2** and the corresponding theoretical curve for **2**.

On the other hand, the frequencies of the IR bands related to the bpa ligand in both compounds are very close to their positions in the free ligand (which are also displayed in Table 4) showing that the pyridyl rings are nearly planar in the complexes. These results are indicative of a similar co-ordination of the ligands to the metallic ions, as expected for isomorphous compounds.

The diffuse reflectance spectrum for compound **1** is typical of octahedral high spin Co(II) complexes. Thus, the UV-VIS spectrum shows three spin-allowed transitions from $^4T_{1g}$ to $^4T_{2g}$ (ν_1 = 9480 cm^{-1}), $^4A_{2g}$ (ν_2 = 18350 cm^{-1}) and $^4T_{1g}$(P) (ν_3 = 20870 cm^{-1}), respectively, the ν_2 transition appearing as a shoulder of ν_3. The values of D_q = 1139 cm^{-1} and B = 606 cm^{-1} which have been calculated from these transitions are typical for high spin Co(II) complexes.[11] The value of B is indicative of 65% covalency of the Co–N bonds in compound **1**. The spectrum also shows a charge-transfer band above 38000 cm^{-1} which could be due to the presence of the four pyridyl rings around the metallic ion.

Magnetic properties

In order to evaluate the magnetic performance of **1** and **2**, molar magnetic susceptibility values, χ_m, were recorded in the 5–300 K range. The χ_m^{-1} curve for **1** has been observed to follow the Curie–Weiss law down to 50 K with values of C_m = 3.50 cm^3 K mol^{-1} (per Co), θ = −16.9 K and g = 2.73. For **2**, the Curie–Weiss law is obeyed across the whole range of temperatures with values of C_m = 4.38 cm^3 K mol^{-1} (per Mn), θ = −0.6 K and g = 2.00.

Fig. 5 displays the thermal variation of the $\chi_m T$ product for **1** and **2**. As observed, the $\chi_m T$ curve for **1** continuously decreases upon cooling from 3.29 cm^3 K mol^{-1} at rt down to 2.45 cm^3 K mol^{-1} at 20 K. At lower temperatures, $\chi_m T$ values increase again up to 2.59 cm^3 K mol^{-1} at 10 K. Upon further cooling, $\chi_m T$ tends to zero. On the other hand, the $\chi_m T$ values for **2** decrease very slowly across the whole range of temperatures from 4.38 cm^3 K mol^{-1} per Mn at rt. As observed, $\chi_m T$ remains practically constant down to 40 K, the $\chi_m T$ value at 5 K being 3.90 cm^3 K mol^{-1}.

The decreasing values of $\chi_m T$ upon cooling indicates the occurrence of antiferromagnetic coupling for **1** and **2**. This magnetic exchange must be attributed to the intermetallic coupling through the bpa bridges, which is expected to be weak as a consequence of the long pathway through this organic ligand. The fact that the slope of the decreasing $\chi_m T$ curve is higher for **1** (Co^{II}) than for **2** (Mn^{II}) is obviously due to the spin–orbit coupling contributing to the decrease of μ_{eff} in the Co^{II} compound.

With the aim of interpreting the magnetic data, eqn. (1)[12] has been used. This expression corresponds to an infinite-spin, linear chain model scaled for S = 5/2, where N and k are the Avogadro and Boltzmann constants, respectively, and β is the Bohr magneton.

$$\chi_m = \frac{Ng^2\beta^2 S(S+1)}{3kT}\left(\frac{1-u}{1+u}\right) \quad (1)$$

$$u = \frac{T}{T_0} - \coth\frac{T}{T_0}; \quad T_0 = \frac{2JS(S+1)}{k}$$

According to eqn. (1), the best fit parameters for compound **2** have been determined to be g = 2.00 (in good agreement with the experimental data) and J = −0.05 cm^{-1}. Similar values of the exchange constant have been found for related M–(*gauche*-bpa)$_2$–M chains.[4a]

For compound **1**, no good fit has been possible due to the contribution of the spin–orbit coupling. On the other hand, the slight increase of the magnetic moment with decreasing temperatures observed between 20 and 10 K deserves some attention. According to the structural features, the occurrence of low-temperature ferromagnetic coupling or canting phenomena are discarded as well as the presence of any kind of impurity. Thus, the occurrence of this anomaly is currently under investigation.

Concluding remarks

Compounds **1** and **2** are very good examples of the high capability of the bpa ligand to be incorporated in structural frameworks. Thus, in these compounds bpa is present in both conformations, *gauche* and *anti*, as chelating ligands and as crystallisation molecules, respectively. This versatility in performance is due to the flexibility of bpa, which adopts py–C–C–py angles as different as 66.3° and 179.0°. The coupling through *gauche*-bpa gives rise to antiferromagnetic interactions for both compounds **1** and **2**.

Acknowledgements

This work has been carried out with the financial support of the Universidad del País Vasco/Euskal Herriko Unibertsitatea (Grant UPV 130310-EB201/1998), the Gobierno Vasco/Eusko Jaurlaritza (Project PI99/53) and the Ministerio de Educación y Cultura (Project PB97-0637). M. L. H. thanks the Universidad del País Vasco/Euskal Herriko Unibertsitatea for grant UPV 130.310.EB234/95. N. P. thanks the Gobierno Vasco/Eusko Jaurlaritza for grant PI99/53.

References

1 (*a*) M. Fujita, Y. J. Kwon, S. Washizu and K. Ogura, *J. Am. Chem. Soc.*, 1994, **116**, 1151; (*b*) M. Kondo, T. Yoshitomi, K. Seki, H. Matsuzaka and S. Kitagawa, *Angew. Chem., Int. Ed. Engl.*, 1997, **36**, 1725; (*c*) J. Lu, T. Paliwala, S. C. Lim, C. Yu, T. Niu and A. J. Jacobson, *Inorg. Chem.*, 1997, **36**, 923; (*d*) M. L. Tong, B. H. Ye, J. W. Cai, X. M. Chen and S. W. Ng, *Inorg. Chem.*, 1998, **37**, 2645; (*e*) M. L. Tong, X. M. Chen, X. L. Yu and T. C. W. Mak, *J. Chem. Soc., Dalton Trans.*, 1998, 5; (*f*) J. Y. Lu, B. R. Cabrera, R.-J. Wang and J. Li, *Inorg. Chem.*, 1999, **38**, 4608; (*g*) J. Y. Lu, M. A. Lawandy, J. Li, T. Yuen and C. L. Lin, *Inorg. Chem.*, 1999, **38**, 2695; (*h*) L.-M. Zheng, X. Fang, K.-H. Lii, H.-H. Song, X.-Q. Xin, H.-K. Fun, K. Chinnakali and I. A. Razak, *J. Chem. Soc., Dalton Trans.*, 1999, 2311; (*i*) Y.-B. Dong, M. D. Smith, R. C. Layland and H.-C. zur Loye, *J. Chem. Soc., Dalton Trans.*, 2000, 775; (*j*) H.-J. Chen, L.-Z. Zhang, Z.-G. Cai, G. Yang and X.-M. Chen, *J. Chem. Soc., Dalton Trans.*, 2000, 2463; (*k*) S.-i. Noro, S. Kitagawa, M. Kondo and K. Seki, *Angew. Chem., Int. Ed.*, 2000, **39**, 2082; (*l*) Z. Shi, S. Feng, S. Gao, L. Zhang, G. Yang and J. Hua, *Angew. Chem., Int. Ed.*, 2000, **39**, 2325; (*m*) J. Tao, M.-L. Tong and X.-M. Chen, *J. Chem. Soc., Dalton Trans.*, 2000, 3669; (*n*) M.-L. Tong, H.-J. Chen and X.-M. Chen, *Inorg. Chem.*, 2000, **39**, 2235.

2 (*a*) R. Robson, B. F. Abrahams, S. R. Batten, R. W. Gable, B. F. Hoskins and J. Liu, *Supramolecular Architecture*, American Chemical Society, Washington, DC, 1992, ch. 19; (*b*) P. Losier and M. J. Zaworotko, *Angew. Chem., Int. Ed. Engl.*, 1996, **35**, 2779; (*c*) M. G. Barandika, M. L. Hernández-Pino, M. K. Urtiaga, R. Cortés, L. Lezama, M. I. Arriortua and T. Rojo, *J. Chem. Soc., Dalton Trans.*, 2000, 1469; (*d*) L. R. MacGillivray, S. Subramanian and M. J. Zaworotko, *J. Chem. Soc., Chem. Commun.*, 1994, 1325; (*e*) O. M. Yahi and H. Li, *J. Am. Chem. Soc.*, 1995, **117**, 10401; (*f*) O. M. Yaghi and G. Li, *Angew. Chem., Int. Ed. Engl.*, 1995, **34**, 207; (*g*) O. M. Yaghi, G. Li and T. L. Groy, *Inorg. Chem.*, 1997, **36**, 4292; (*h*) L. Carlucci, G. Ciani, D. M. Proserpio and A. Sironi, *J. Chem. Soc., Chem. Commun.*, 1994, 2755; (*i*) D. Hagrman, R. P. Hammond, R. Haushalter and J. Zubieta, *Chem. Mater.*, 1998, **10**, 2091; (*j*) A. J. Blake, N. R. Champness, S. S. M. Chung, W. Li and M. Schröder, *Chem. Commun.*, 1997, 1005; (*k*) A. J. Blake, N. R. Champness, A. Khlobystov, D. A. Lemenovskii, W. Li and M. Schröder, *Chem. Commun.*, 1997, 2027; (*l*) G. De Munno, T. Poerio, G. Viau, M. Julve, F. Lloret, Y. Journaux and E. Riviere, *Chem. Commun.*, 1996, 2587; (*m*) A. J. Blake, S. J. Hill, P. Hubberstey and W. S. Li, *J. Chem. Soc., Dalton Trans.*, 1998, 909; (*n*) T. O. S. Jung, S. H. Park, D. C. Kim and K. M. Lim, *Inorg. Chem.*, 1998, **37**, 610; (*o*) L. Carlucci, G. Ciani, D. M. Proserpio and A. J. Sironi, *J. Chem. Soc., Dalton Trans.*, 1997, 1801; (*p*) J. A. Real, E. Andrés, M. C. Muñoz, M. Julve, T. Granier, A. Bousseksou and F. Varret, *Science*, 1995, **268**, 265; (*q*) G. De Munno, D. Armentano, T. Poerio, M. Julve and J. A. Real, *J. Chem. Soc., Dalton Trans.*, 1999, 1813; (*r*) O.-S. Jung, S. O. Park, K. M. Kim and H. G. Jang, *Inorg. Chem.*, 1998, **37**, 5781; (*s*) Y.-B. Dong, R. C. Layland, M. D. Smith, N. G. Pschirer, U. H. F. Bunz and H.-C. zur Loye, *Inorg. Chem.*, 1999, **38**, 3056; (*t*) M. J. Plater, M. R. St. J. Foreman, T. Gelbrich and M. B. Hursthouse, *J. Chem. Soc., Dalton Trans.*, 2000, 1995.

3 (*a*) T. L. Hennigar, D. C. MacQuarrie, P. Losier, R. D. Rogers and M. J. Zaworotko, *Angew. Chem., Int. Ed. Engl.*, 1997, **36**, 972; (*b*) K. N. Power, T. L. Hennigar and M. Zaworotko, *Chem. Commun.*, 1998, 595; (*c*) C. S. Hong and Y. Do, *Inorg. Chem.*, 1998, **37**, 4470; (*d*) M. Ferbinteanu, G. Marinescu, H. W. Roesky, M. Noltemeyer, H.-G. Schmidt and M. Andruh, *Polyhedron*, 1998, **18**, 243; (*e*) M. Fujita, Y. J. Kwon, M. Miyazawa and K. Ogura, *J. Chem. Soc., Chem. Commun.*, 1994, 1977; (*f*) Y.-B. Dong, M. D. Smith, R. C. Layland and H.-C. zur Loye, *Inorg. Chem.*, 1999, **38**, 5027; (*g*) Y. B. Dong, R. C. Layland, M. D. Smith, N. G. Pschirer, U. H. F. Bunz and H.-C. zur Loye, *Inorg. Chem.*, 1999, **38**, 3056; (*h*) C. S. Hong, S.-K. Son, Y. S. Lee, M.-J. Jun and Y. Do, *Inorg. Chem.*, 1999, **38**, 5602; (*i*) Q.-M. Wang, G.-C. Guo and T. C. W. Mak, *Chem. Commun.*, 1999, 1849; (*j*) L. Carlucci, G. Ciani, D. M. Proserpio and S. Rizzato, *Chem. Commun.*, 2000, 1319; (*k*) M. Kondo, M. Shimamura, S. Noro, Y. Kimura, K. Uemura and S. Kitagawa, *J. Solid State Chem.*, 2000, **152**, 113.

4 (*a*) M. L. Hernández, M. G. Barandika, M. K. Urtiaga, R. Cortés, L. Lezama, M. I. Arriortua and T. Rojo, *J. Chem. Soc., Dalton Trans.*, 1999, 1401; (*b*) M. L. Hernández, M. G. Barandika, M. K. Urtiaga, R. Cortés, L. Lezama and M. I. Arriortua, *J. Chem. Soc., Dalton Trans.*, 2000, 79.

5 G. M. Sheldrick, SHELXS97, Program for the Solution of Crystal Structures, University of Göttingen, Germany, 1997.

6 G. M. Sheldrick, SHELXL97, Program for the Refinement of Crystal Structures, University of Göttingen, Germany, 1997.

7 D. T. Cromer and J. T. Waber, *International Tables for X-Ray Crystallography*, Vol. IV, Kynoch Press, Birmingham, 1974.

8 J. Rodriguez-Carvajal, FULLPROF, Program for Rietveld Pattern Matching Analysis of Powder Patterns, 1997 (see: http://www-llb.cea.fr/fullweb/winplotr/winplotr.htm).

9 (*a*) H. M. Rietveld, *Acta Crystallogr.*, 1967, **12**, 151; (*b*) H. M. Rietveld, *J. Appl. Crystallogr.*, 1969, **6**, 65.

10 K. Nakamoto, *Infrared Spectra of Inorganic and Coordination Compounds*, John Wiley & Sons, New York, 1997.

11 A. B. P. Lever, *Inorganic Electronic Spectroscopy*, Elsevier Science B.V., Amsterdam, Netherlands, 1984.

12 M. E. Fisher, *Am. J. Phys.*, 1964, **32**, 343.

13 C. K. Johnson, ORTEP, Report ORNL-5138, Oak Ridge National Laboratory, Oak Ridge, TN, 1976.